Front. Optoelectron. 2017, 10(2): 180–188
DOI 10.1007/s12200-017-0711-y

RESEARCH ARTICLE

Theoretical demonstration of all-optical switchable and tunable UWB doublet pulse train generator utilizing SOA wavelength conversion and tunable time delay

Zhefeng HU (✉), Jianhui XU, Min HOU

School of Communication and Information Engineering, University of Electronic Science and Technology of China, Chengdu 611731, China

© Higher Education Press and Springer-Verlag Berlin Heidelberg 2017

Abstract An all-optical ultrawide band (UWB) doublet pulse train signal generator is proposed and theoretically simulated by utilizing an inverse wavelength conversion base on the cross-gain modulation (XGM) effect in a semiconductor optical amplifier (SOA) and controllable time delay in two optical delay lines (ODLs). The proposed scheme is not only optically switchable in the polarity of pulse by switching the polarity of input pulse but also tunable in signal pulse width and radiofrequency (RF) spectrum by tuning the ODLs.

Keywords microwave photonics, ultrawide band (UWB), tunable, switchable, semiconductor optical amplifier (SOA), tunable time delay

1 Introduction

Ultrawide band (UWB) is regarded as an important technology with wide applications in numerous fields, such as sensing networks in broadband and space communication systems with high capacity and short range [1]. The frequency band of UWB from 3.1 to 10.6 GHz has been assigned for use without license by the US Federal Communications Commission (FCC), which must occupy larger than 20% in fractional bandwidth or greater than 500 MHz in bandwidth at 10 dB [2]. In practical applications, devices are preferred because they can obtain switchability in pulse polarity and tunability in signal pulse width and radiofrequency (RF) spectrum.

This technology is typically used for short-distance communication networks, such as local area network (LAN) and personal area network (PAN), because UWB signal experiences remarkable loss in free-space transmission. The generation of UWB signal in an optical domain has been extensively investigated because of low loss transmission over long distance through optical fibers. Numerous schemes have been demonstrated using electro-optical [3–5] and all-optical [6–10] methods. In particular, schemes that generate UWB monocycle signal switchable in the polarity of pulse and tunable in signal pulse width and RF spectrum have been demonstrated by utilizing a semiconductor optical amplifier (SOA) as a wavelength converter and an optical delay line (ODL) or a dispersive fiber to obtain controllable time delay [8–10]. Nevertheless, generating UWB signal in higher order with a tunable and switchable property is still difficult.

In this study, a novel generation scheme of all-optical tunable and switchable UWB doublet pulse train is proposed and simulated through wavelength conversion based on a cross-gain modulation (XGM) effect in an SOA and controllable time delay through two ODLs. The system is optically switchable in the polarity of pulse and tunable in signal pulse width and RF spectrum.

2 Operation principle

Figure 1 illustrates the working principle of the proposed all-optical UWB doublet signal generation scheme with switchable and tunable property. In Fig. 1 (a), a pulse train in Gaussian shape at wavelength λ_s is injected as the pump signal light. This pump signal is merged by a wavelength division multiplexer (WDM) with two continuous waves (CWs) at wavelengths λ_{p1} and λ_{p2} as the input of an SOA. Two pulse trains are modulated in polarity-reversed Gaussian shape on the probe wavelengths at the output of the SOA through the XGM effect. The pulse train in the

Received March 10, 2017; accepted April 26, 2017

E-mail: zfhu@uestc.edu.cn

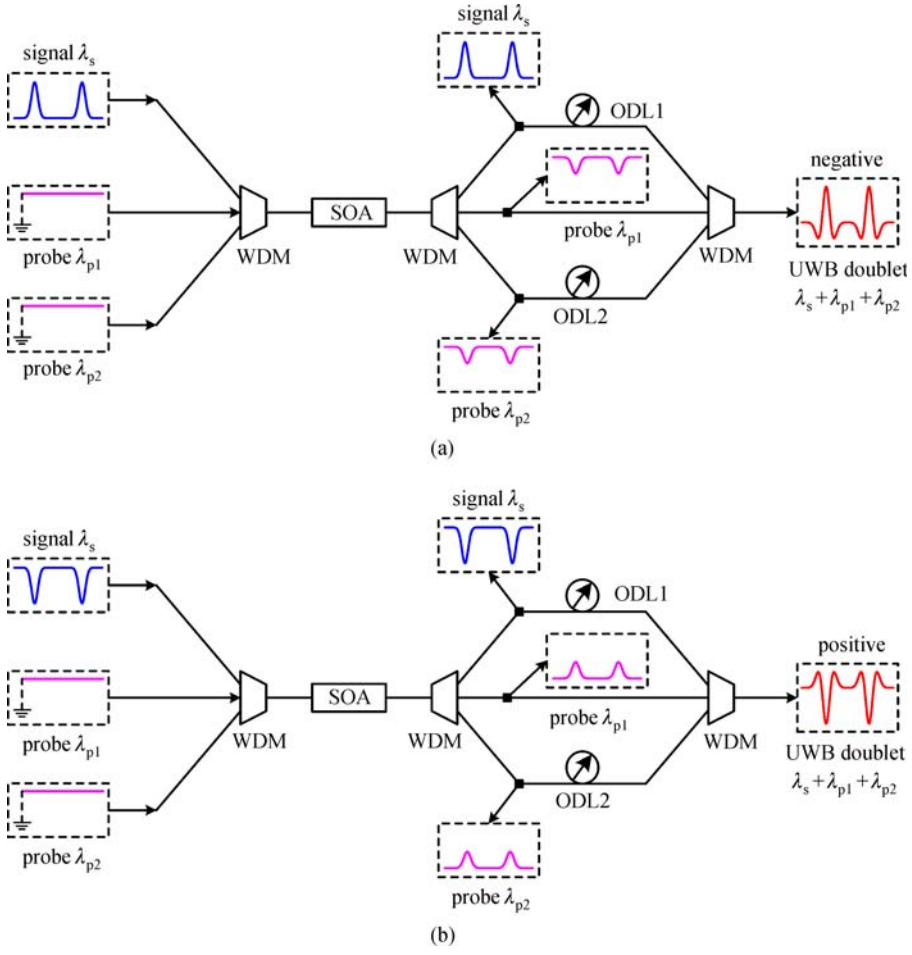

Fig. 1 Working principle of the proposed switchable and tunable UWB pulse train generation scheme. (a) UWB pulse train in a negative doublet shape; (b) UWB pulse train in a positive doublet shape

Gaussian shape and those in the polarity-reversed Gaussian shape are demultiplexed into three different lights by another WDM. Two ODLs on the paths of signal wavelength λ_s and probe wavelength λ_{p2} are employed to introduce time delay with different values. Afterward, a third WDM is used to merge the output pump signal and the modulated the probes again. In this manner, an optical UWB signal in a doublet shape on the mixed light is obtained. In Fig. 1(b), the signal pulse train is switched to polarity-reversed Gaussian shape. As such, two pulse trains in Gaussian shape are achieved on output probe wavelengths. In a similar process, a UWB pulse train in a positive doublet shape is found on the mixed light.

The signal pulse width of the final output UWB pulse train in a doublet shape can be tuned because the time delays among the output pulse trains on the signal and probe wavelengths can be controlled by adjusting the two ODLs. Moreover, the generated UWB pulse train can be switched between negative and positive doublet shapes when the input signal pulse train is switched between the Gaussian and the polarity-reversed Gaussian shape.

3 Theoretical model and simulation parameters

The carrier rate equation and light propagation should be introduced in Eq. (1) to describe the process of XGM effect that occurred in the SOA [11]:

$$\begin{cases} \dfrac{\partial N}{\partial t} = \dfrac{I}{eV} - R(N) - \displaystyle\sum_{\omega=\mathrm{s,p1,p2}} \dfrac{\Gamma g_\omega(N)}{A_0 hc/\lambda_\omega}|A_\omega|^2, \\ \dfrac{\mathrm{d}A_\omega}{\mathrm{d}z} = [\Gamma g_\omega(N)(1-\mathrm{i}\alpha) - \alpha_{\mathrm{int}}]A_\omega, \end{cases} \tag{1}$$

where carrier density, injection current, quantity of electron charge, volume, and cross-section of the active region are represented as N, I, e, V, and A_0, respectively. The gain coefficient and photon energy of lights at wavelength λ_ω are represented as $g_\omega(N)$ and hc/λ_ω, respectively. The index ω corresponds to signal(s) and two probes (p1 and p2). Carrier consumption caused by radiative and nonradiative recombination are accounted as $R(N)$. The amplitudes of lights at wavelength λ_ω is expressed as A_ω.

The recombination rate can be expressed by the following equation depending on carrier density:

$$R(N) = AN + BN^2 + CN^3. \quad (2)$$

If the peak wavelength, which is assumed to shift linearly with carrier density, i.e., $\lambda_N = \lambda_0 - a_4(N - N_0)$, is represented as λ_N, we can express the gain coefficient as follows:

$$g_\omega(N,\lambda_\omega) = a_1(N-N_0) - a_2(\lambda_\omega - \lambda_N)^2 + a_3(\lambda_\omega - \lambda_N)^3. \quad (3)$$

Table 1 lists the description and value of SOA parameters used in the simulation, where $V = lwd$ and $A_0 = wd$. λ_s, λ_{p1}, and λ_{p2} are 1550, 1560, and 1540 nm, respectively.

Table 1 Parameters of SOA used in simulation

symbol	description	value
l	active region length	10^{-3} m
w	active region width	1.5×10^{-6} m
d	active region thickness	2×10^{-7} m
A	coefficient of unimolecular recombination	1.5×10^{8} s^{-1}
B	coefficient of bimolecular recombination	1×10^{-16} m^3/s
C	coefficient of Auger recombination	1.2×10^{-40} m^6/s
a_1	gain coefficient 1	5×10^{-20} m^2
a_2	gain coefficient 2	7.4×10^{18} m^{-3}
a_3	gain coefficient 3	3.155×10^{25} m^{-4}
a_4	gain coefficient 4	3×10^{-32} m^4
N_0	transparency carrier density	1×10^{24} m^{-3}
λ_0	transparency wavelength	1.56×10^{-6} m
α	linewidth enhancement factor	4
α_{int}	internal loss	5×10^{3} m^{-1}
Γ	confinement factor	0.3

4 Results and discussion

The temporal traces of pulse trains on different wavelengths at the input and output side of the SOA are displayed in Fig. 2 with an input signal corresponding to a Gaussian pulse train whose repetition rate is 1.25 GHz and full width at half maximum (FWHM) is 70 ps. The

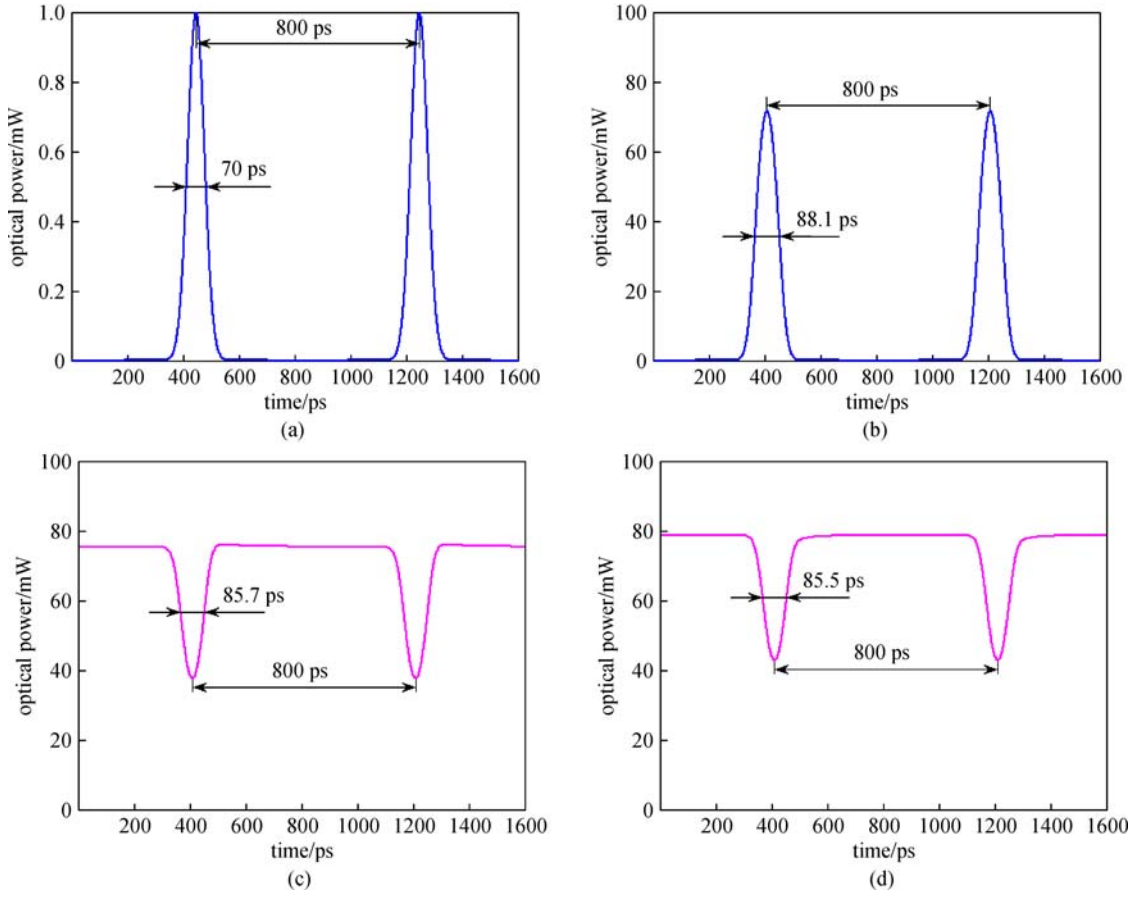

Fig. 2 Temporal trace of lights at different wavelengths when the input signal is a Gaussian pulse train. (a) Input signal; (b) output signal; (c) output probe at λ_{p1}; (d) output probe at λ_{p2}

FWHMs of the output lights on signal and probe wavelengths are 88.1, 85.7, and 85.5 ps, respectively. The input powers of the pump and two probe lights are 1, 0.6, and 0.6 mW.

The temporal traces of pulse trains on different wavelengths at the input and output side of the SOA are displayed in Fig. 3 with an input signal of a polarity-reversed Gaussian pulse train whose repetition rate is 1.25 GHz and FWHM is 70 ps. The FWHM of the output signal and probes are 55.3, 51.9, and 53.6 ps, respectively.

The waveforms of the generated UWB signals are shown in Fig. 4, while the time delay of ODL1 is controlled at different amounts. Throughout the operation process, the time delay caused by ODL2 is controlled as twice as the value of the time delay caused by ODL1. In Figs. 4 (a)–4(c), a Gaussian pulse train is used as the input signal. After time delays are introduced, each Gaussian pulse in the output signal pulse train is adjusted in the middle of two polarity-reversed Gaussian pulses in the output probe pulse trains. Our results reveal a UWB pulse train in which each pulse exhibits a negative doublet shape in the final output. In Figs. 4(d)–4(f), a polarity-reversed Gaussian pulse train is used as the input signal, that is, each polarity-reversed Gaussian pulse in the output signal pulse train is adjusted in the middle of two Gaussian pulses in the output probe pulse trains. As such, the UWB signal is produced in a positive doublet shape at the final output.

The amplification and wavelength conversion in SOA are not perfect. Nonlinear effects, such as XGM and cross-phase modulation (XPM), likely cause a slight distortion in pulse shape. Consequently, Gaussian and polarity-reversed Gaussian pulses are not absolutely symmetric. The overlap becomes heavy when the time delay is small. Thus, the left and right peaks may vary (Fig. 4 (d)).

In Figs. 2 and 3, the pulse widths of the generated probe pulses are almost equal. However, the output signal pulse is asymmetric and thus results in different left and right FWHMs when the time delay is small, that is, the overlap of pulses is heavy. However, the overlap becomes slight when the time delay is large, and the same left and right FWHMs appear.

The dependence of the generated UWB doublet pulse widths on time delay caused by ODL1 are plotted in Fig. 5. The FWHMs of the left, center, and right parts of the generated UWB signal in a negative doublet shape can vary from 44.2 to 80.8 ps, 57.8 to 85.7 ps, and 42.8 to 80.7

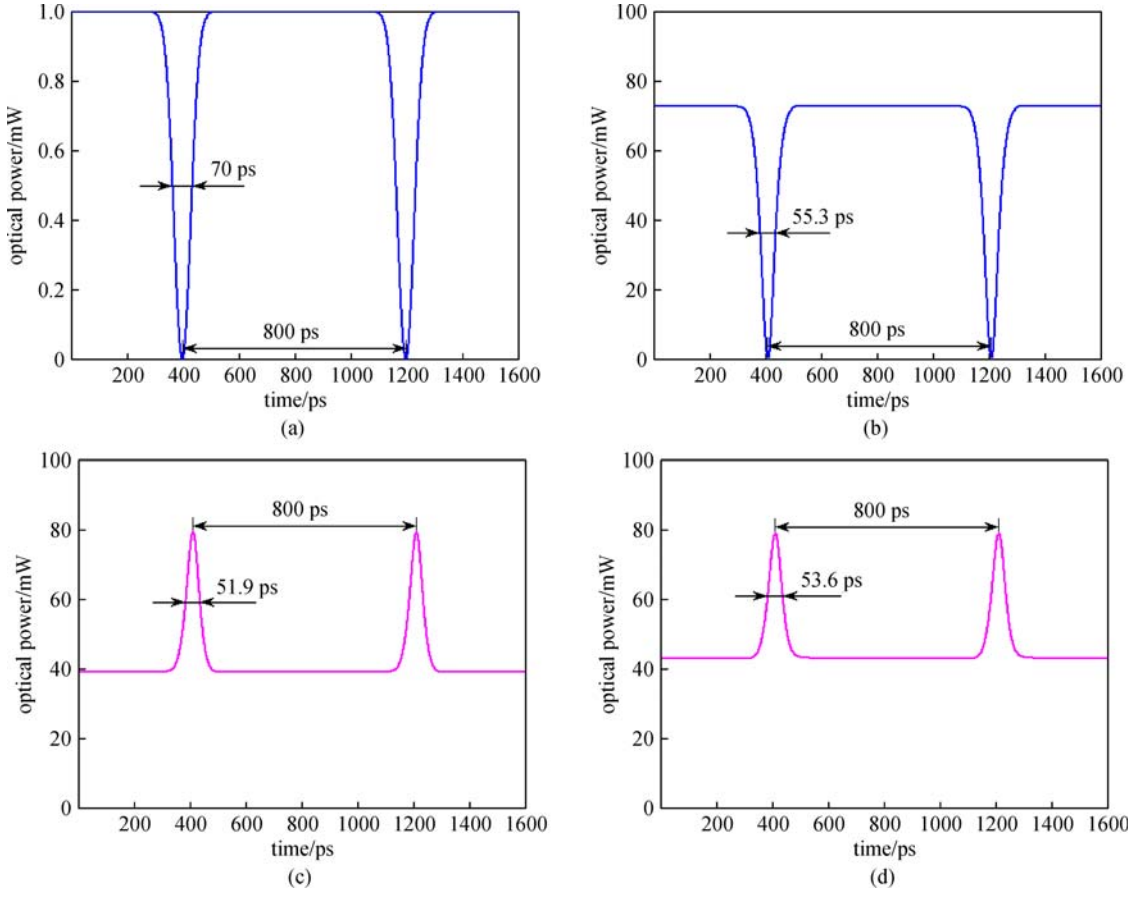

Fig. 3 Temporal trace of lights at different wavelengths when the input signal is a polarity-reversed Gaussian pulse train. (a) Input signal; (b) output signal; (c) output probe at λ_{p1}; (d) output probe at λ_{p2}

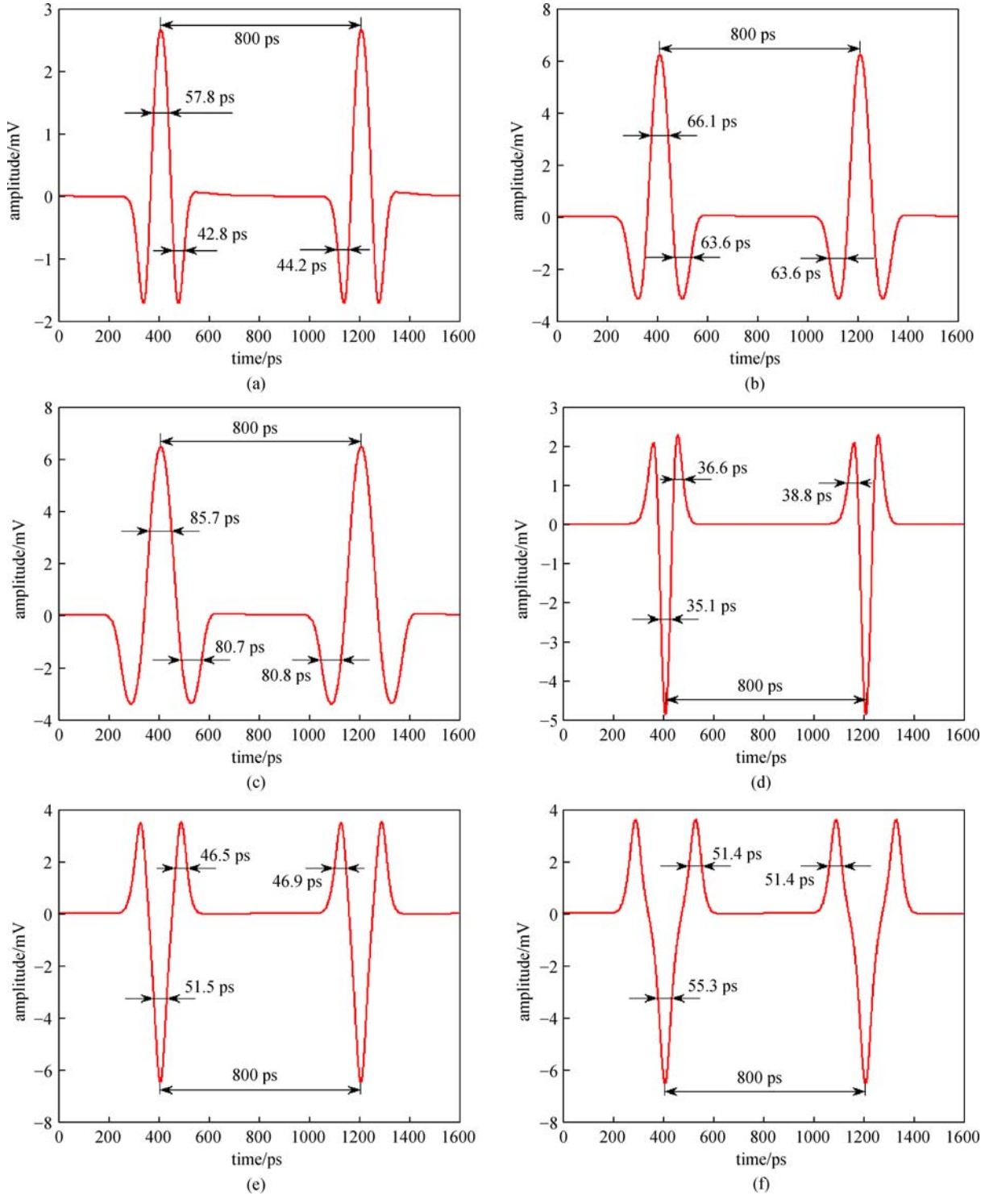

Fig. 4 Waveforms of the obtained UWB signal in doublet shape with time delay introduced by ODL1 tuned at different values. (a)–(c) 40, 80, and 120 ps (UWB signals in negative doublet shape); (d)–(f) 40, 80, and 120 ps (UWB signals in positive doublet shape)

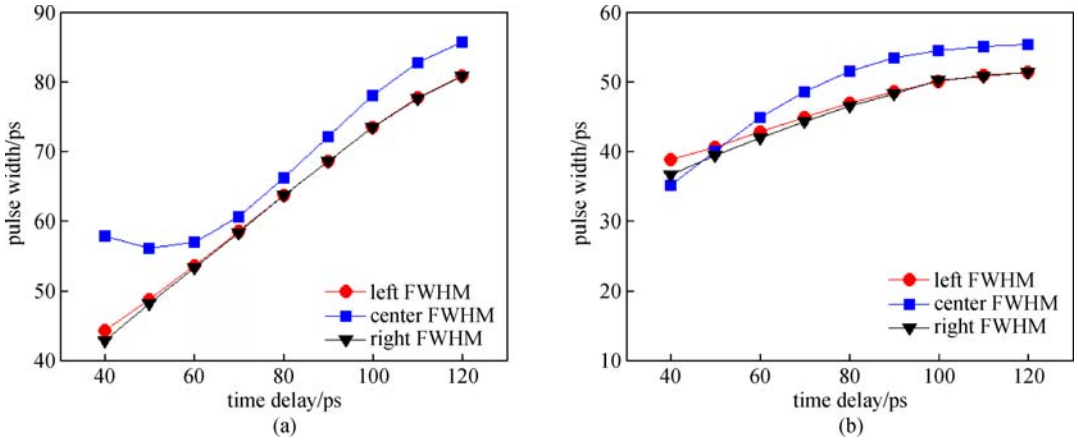

Fig. 5 Pulse widths depending on time delay of ODL1. (a) UWB signals in negative doublet shape; (b) UWB signals in positive doublet shape

ps, respectively (see Fig. 5(a)). For the generated UWB signal in the positive doublet shape, the corresponding parameters can change from 38.8 to 51.4 ps, 35.1 to 55.3 ps, and 36.6 to 51.4 ps, respectively (see Fig. 5(b)).

The FWHM of the output signal in the Gaussian shape is 88.1 ps (44.05 ps for a half pulse width) because Gaussian and polarity-reversed Gaussian pulses on the output signal and probes are not absolutely symmetric. The peaks of the probe pulses remarkably affect the center FWHM of the final output signal when the time delay is small (40 to 60 ps). As such, the value abnormal changes.

The RF spectra of the generated signals and their envelopes are shown in Fig. 6 to verify the successful generation of the UWB doublet signal. Figure 6 illustrates a repetition frequency of 1.25 GHz of the output UWB doublet signal.

Figure 7 denotes the RF spectrum variation with time delay changes caused by ODL1. In the experiment, the central frequency, bandwidth at 10 dB, and fractional bandwidth of the generated UWB signal in the negative doublet shape can be varied from 6.22 to 3.75 GHz, 7.68 to 4.76 GHz, and 123.5% to 126.9%, respectively. For the UWB signal in a positive doublet shape, these parameters can be changed from 8.82 to 3.92 GHz, 11.77 to 4.89 GHz, and 133.4% to 124.7%, respectively. We note that the RF spectra of the realized signals fit the UWB definition of FCC quite well.

The pulses of the output signal and probes from SOA are narrower when the input signal is in polarity-reversed Gaussian shape. Under this condition, the left and right peaks possibly influence the final shape and consequently exhibit more remarkable changes in the pulse width of the positive doublet than in the negative doublet. As such, the spectrum parameters are also altered.

The central frequency and 10 dB bandwidth of the negative doublet almost isometrically change because of the mild overlap and thus slight alter the fractional bandwidth. However, the 10 dB bandwidth of the positive doublet decreases more rapidly than the central frequency does when time delay increases. As a result, this phenomenon decreases the fractional bandwidth.

Analyzing the simulation results shown in Figs. 4, 5, 6, and 7, we discover that the left, central, and right FWHMs of the generated UWB signal in doublet shape increase when the time delay caused by ODL1 increase. Conversely, the center FWHM of the UWB signal in the negative doublet shape slightly decreases when the time delay is small, but the central frequency and bandwidth at 10 dB decrease. In this manner, the tunability in signal pulse width and RF spectrum is obtained for the generated UWB signal in doublet shape by adjusting the time delay caused by ODL1 and ODL2. Moreover, switchability in the polarity of pulse can be achieved by switching the input signal between Gaussian pulse train and polarity-reversed Gaussian pulse train.

The proposed all-optical switchable UWB doublet signal generation scheme can be conveniently applied to the pulse polarity modulation (PPM) scheme for all-optical UWB signal transmission and the PPM is regarded as an essential modulation method for the application of UWB signals [12]. The optical tunability characteristic of the proposed UWB doublet signal generation scheme provides the facilities for signal pulse width and RF band control in a practical and flexible application system.

5 Conclusions

We proposed and theoretically simulated an all-optical UWB doublet signal generation scheme that exhibits not only an optically switchable property in the polarity of pulse but also a tunable characteristic in signal pulse width and RF spectrum. The parameters of the signal pulse width, central frequency, and bandwidth at 10 dB of the generated UWB signal in doublet shape can be conveniently tuned by adjusting the time delay of ODLs. The

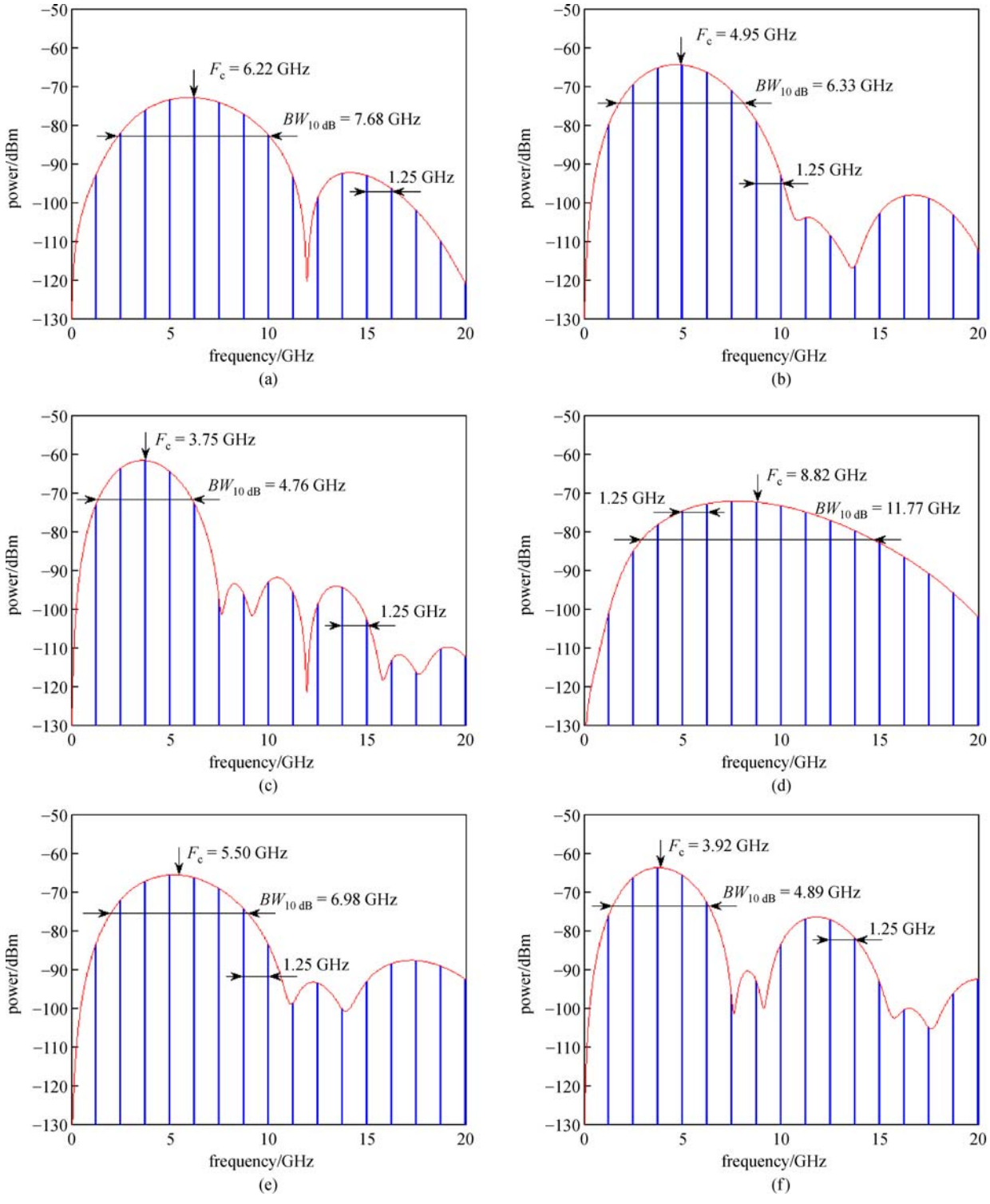

Fig. 6 RF spectra of the generated signals and their envelopes in doublet shape with time delay introduced by ODL1 tuned at different values. (a)–(c) 40, 80, and 120 ps (UWB signals in negative doublet shape); (d)–(f) 40, 80, 120 ps (UWB signals in positive doublet shape). F_c: central frequency; $BW_{10\ dB}$: bandwidth at 10 dB

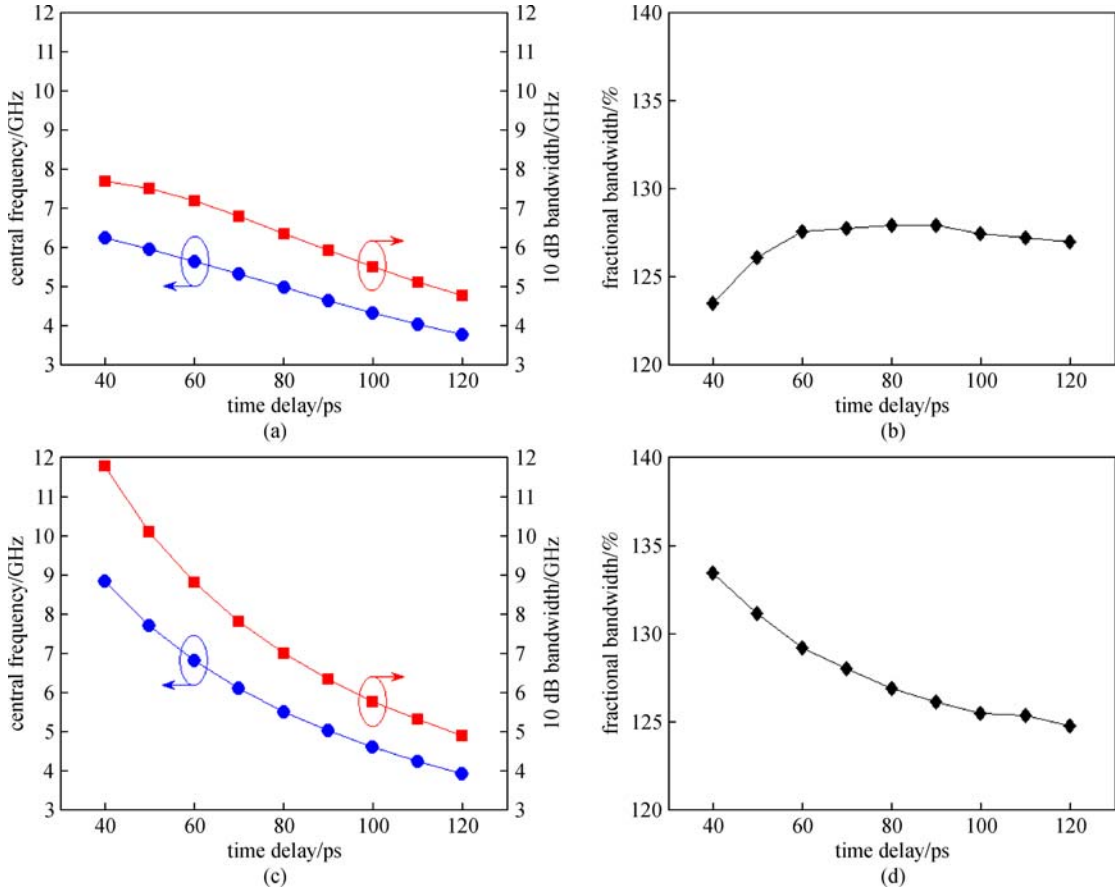

Fig. 7 Central frequency, 10 dB bandwidth, and fractional bandwidth depending on the time delay of ODL1. (a) and (b) UWB signal in negative doublet shape; (c) and (d) UWB signal in positive doublet shape. (a) and (c) central frequency and 10 dB bandwidth; (b) and (d) fractional bandwidth

proposed UWB doublet signal generator provides a potential approach in PPM scheme for all-optical UWB signal transmission and flexibility for UWB applications.

Acknowledgements This work was supported by the National Natural Science Foundation of China (Grant Nos. 61501088, 61307088, 61505020, and 61675040), the Joint Funds of the National Natural Science Foundation of China (Grant No. U1633129), the Science and Technology Planning Project of Sichuan Province (No. MZ2016036), and the Fundamental Research Funds for the Central Universities (Nos. ZYGX2016J003, ZYGX2016J005, and ZYGX2016J009).

References

1. Porcino D, Hirt W. Ultra-wideband radio technology: potential and challenges ahead. IEEE Communications Magazine, 2003, 41(7): 66–74
2. Aiello G R, Rogerson G D. Ultra-wideband wireless systems. IEEE Microwave Magazine, 2003, 4(2): 36–47
3. Zeng F, Yao J. Ultrawideband impulse radio signal generation using a high-speed electrooptic phase modulator and a fiber-Bragg-grating-based frequency discriminator. IEEE Photonics Technology Letters, 2006, 18(19): 2062–2064
4. Wang Q, Yao J. Switchable optical UWB monocycle and doublet generation using a reconfigurable photonic microwave delay-line filter. Optics Express, 2007, 15(22): 14667–14672
5. Wang Q, Yao J. An electrically switchable optical ultrawideband pulse generator. Journal of Lightwave Technology, 2007, 25(11): 3626–3633
6. Shao J, Sun J. Filter-free ultra-wideband doublet pulses generation based on wavelength conversion and fiber dispersion effect. Optics Communications, 2012, 285(12): 2790–2793
7. Shao J, Liu S. Photonic generation of filter-free ultrawideband monocycle and doublet signal using single semiconductor optical amplifier in counter-propagation scheme. Optical Engineering, 2016, 55(2): 026117
8. Hu Z, Sun J, Shao J, Zhang X. Filter-free optically switchable and tunable ultrawideband monocycle generation based on wavelength conversion and fiber dispersion. IEEE Photonics Technology Letters, 2010, 22(1): 42–44
9. Hu Z, Sun J, Shao J. Simulation of optically switchable and tunable ultrawideband monocycle generation using semiconductor optical amplifier and optical delay line. In: Photonics and Optoelectronics Meetings (POEM) 2009. Proceedings of the Society for Photo-

Instrumentation Engineers, 2009, 7516: 75160Q
10. Hu Z, Xu J, Hou M. Proposal for all-optical switchable and tunable ultrawideband monocycle generation utilizing SOA wavelength conversion and time delay. Photonic Sensors, 2017, 7(1): 66–71
11. Hsieh J, Gong P, Lee S, Wu J. Improved dynamic characteristics on four-wave mixing wavelength conversion in light-holding SOAs. IEEE Journal of Selected Topics in Quantum Electronics, 2004, 10 (5): 1187–1196
12. Yao J, Zeng F, Wang Q. Photonic generation of ultrawideband signals. Journal of Lightwave Technology, 2007, 25(11): 3219–3235

Zhefeng Hu received his Ph.D. degree in electronic science and technology, at Huazhong University of Science and Technology in 2010. From 2013 to 2014, he was a post-doctoral research fellow at the University of Padova. He is currently an Associate Professor at University of Electronic Science and Technology of China. His research interests focus on optoelectronic devices, microwave photonics and optics communications.

Jianhui XU received the B.S. degree in Chongqing University of Posts and Telecommunications in 2015. Now he researches on optical communication at University of Electronic Science and Technology of China.

Min Hou is purchasing her Master degree in optical engineering at the University of Electronic Science and Technology of China. Her research focuses on fiber-optic nonlinear effects.